



HAL
open science

Highly stable Ni/ZnO-Al₂O₃ adsorbent promoted by TiO₂ for reactive adsorption desulfurization

Bowen Liu, Peng Bai, Yang Wang, Zhun Dong, Pingping Wu, Svetlana Mintova, Zifeng Yan

► To cite this version:

Bowen Liu, Peng Bai, Yang Wang, Zhun Dong, Pingping Wu, et al.. Highly stable Ni/ZnO-Al₂O₃ adsorbent promoted by TiO₂ for reactive adsorption desulfurization. *EcoMat*, 2021, 3 (4), 10.1002/eom2.12114 . hal-03414925

HAL Id: hal-03414925

<https://hal.science/hal-03414925>

Submitted on 4 Nov 2021

HAL is a multi-disciplinary open access archive for the deposit and dissemination of scientific research documents, whether they are published or not. The documents may come from teaching and research institutions in France or abroad, or from public or private research centers.

L'archive ouverte pluridisciplinaire **HAL**, est destinée au dépôt et à la diffusion de documents scientifiques de niveau recherche, publiés ou non, émanant des établissements d'enseignement et de recherche français ou étrangers, des laboratoires publics ou privés.

Highly stable Ni/ZnO-Al₂O₃ adsorbent promoted by TiO₂ for reactive adsorption desulfurization

Bowen Liu[†], Peng Bai^{†,*}, Yang Wang[†], Zhun Dong[†], Pingping Wu[†], Svetlana Mintova^{†,‡} and Zifeng Yan[†]

[†] State Key Laboratory of Heavy Oil Processing, Key Laboratory of Catalysis, College of Chemical Engineering, China University of Petroleum (East China), Qingdao 266580, China
E-mail: baipeng@upc.edu.cn

[‡] Normandie University, ENSICAEN, UNICAEN, CNRS, Laboratory of Catalysis and Spectrochemistry, 14000 Caen, France

Keywords: Ni/ZnO-Al₂O₃ adsorbents; Reactive adsorption desulfurization; Stability; ZnAl₂O₄ spinel; TiO₂.

Abstract

The reactive adsorption desulfurization is an important and efficient technology for the ultra-deep desulfurization of gasoline. The performance of an adsorbent is vital for the efficiency of the reactive adsorption desulfurization process. In the case of Ni/ZnO-Al₂O₃ adsorbent, the formation of inert ZnAl₂O₄ spinels is commonly recognized for the deactivation of adsorbents. To solve this problem, in this work, TiO₂ was incorporated in the Ni/ZnO-Al₂O₃ adsorbent by a wet impregnation method to inhibit the formation of spinel structures during the reaction and regeneration processes. The TiO₂ formed a stable protection layer on the surface of Al₂O₃ preventing the interaction between Al₂O₃ and ZnO, which inhibited the formation of ZnAl₂O₄ spinel phase. The reactive adsorption desulfurization performance of the adsorbents was evaluated in a fixed bed reactor using thiophene in n-octane as a model fuel. Evaluation results indicated that the introduction of TiO₂ could significantly improve the stability of the adsorbents during cyclic hydrothermal treatments, while the sulfur capacity slightly dropped. Characterization results revealed that TiO₂ was homogeneously dispersed on the surface of Al₂O₃ support and the incorporation of TiO₂ could maintain a certain amount of Lewis acid sites in the adsorbents, which are favorable for the adsorption of organo-sulfur compounds.

1. Introduction

The air pollution problems which could bring environmental disasters and damages to human health have aroused global concern.¹⁻³ Different types of techniques have been used to eliminate or control the air pollutants (NO_x, SO₂, hydrocarbon, etc.) from vehicle emissions.⁴ The ultra-deep desulfurization technology is effectively used to remove the sulfur compounds from fuel oils.⁵⁻⁹ As fuel oils will remain as the main energy source for vehicles in recent decades,¹⁰ the development of efficient desulfurization technologies is still important due to the more stringent environmental regulations for clean fuel oils.^{11,12} Due to its advantages of low octane loss, low hydrogen consumption and mild operation conditions, the reactive adsorption desulfurization (RADS) technique has become a commercial process named as S-Zorb to produce clean gasoline of Stage V (less than 10 µg/g Sulfur) in China.¹³⁻¹⁷

A RADS mechanism has been widely accepted for the Ni/ZnO catalyst system where the S atom in the organic sulfur compounds firstly reacts with Ni (active site for the catalytic hydrogenolysis of C-S bond) and generates Ni₃S₂. In the presence of H₂, Ni₃S₂ will be converted to H₂S and the Ni sites are restored to Ni⁰. The formed H₂S reacts with ZnO which is the sulfur acceptor to produce ZnS.¹⁸ After combustion (regeneration process) in the air, ZnO is regenerated to complete a RADS-regeneration cycle.¹⁹ The study on the RADS reaction kinetics of Ni/ZnO based adsorbents revealed that the sulfur diffusion in ZnO was identified as the rate-determining step after partial sulfidation of ZnO, and the high dispersion of ZnO and NiO particles was favorable for the reaction.²⁰⁻²² To enhance the dispersion of Ni and ZnO, different supports have been introduced into the Ni/ZnO-based catalysts, such as Al₂O₃, ZrO₂, SiO₂, zeolites.²³⁻²⁵ Among the supports being used, Al₂O₃ is the most common one because of its intrinsic advantages, such as high surface area, low cost and high chemical/mechanical stabilities, triggering extensive interests about the Ni/ZnO-Al₂O₃ adsorbents. Gao et al.²⁶⁻²⁸ investigated the reactivity and regeneration characteristics of the

Ni/ZnO-SiO₂-Al₂O₃. It was found that the inactive ZnAl₂O₄ spinel formed in the reduction and reaction processes significantly decreased the desulfurization activity of adsorbents. Moreover, surface Lewis acid sites increased the activity of the adsorbents because the sulfur-containing compounds bearing lone pair electrons are adsorbed on the adsorbent via the Lewis acid-base interaction.

In our previous studies, a series of Ni/ZnO-Al₂O₃ adsorbents were prepared by a homogeneous precipitation method and a cation-anion double hydrolysis (CADH) method.²⁹⁻³¹ In all these adsorbents, the formation of the inert gahnite phase (such as zinc aluminate) during the reaction was commonly observed, leading to the decrease of activity and fragmentation of adsorbents, which could not be overcome by simply changing the preparation methods.³² The current adsorbents regeneration process can remove the carbon deposits and convert the ZnS into ZnO via burning in the air. But the formation of the spinel phase is irreversible and the burning process would also promote the formation and growth of spinels, especially under steaming conditions of the regeneration process.³³ Besides, for the preparation of industrial adsorbents, to achieve a stable adsorption performance, the adsorbents are usually prepared by the kneading method followed by an aging process to reduce the initial activity, which requires a hydrothermal treatment under the high-temperature steaming conditions.³⁴ The high-temperature steaming conditions in the aging process would also promote the formation of spinel phase.³⁵ Meng et al.²³ found that the presence of ZnAl₂O₄ could reduce the reducibility and activity of the adsorbents, and the high stability of spinel renders it difficult to be removed once it formed. Moreover, the spinel formation also deteriorated the mechanical strength of the adsorbents.³⁶ After deactivation, the difficulties and high cost for recycling result in the fact that most of the spent adsorbents are buried directly, which would cause soil and water pollution.³⁷ Hence, from the sustainable

development point of view, it is highly desirable to develop stable RADS adsorbents via cost-effective approaches.

In order to inhibit the formation of the ZnAl_2O_4 phase, it is a wise way to weaken the interaction between ZnO and Al_2O_3 by introducing a promoter into the adsorbent.^{38,39} Titania has been a common chemical material used as a promoter for the alumina supported catalysts, the synergetic effect of TiO_2 - Al_2O_3 could promote the dispersion of active species and restrain the interaction between active species and Al_2O_3 .^{40,41} Ni/TiO_2 - Al_2O_3 catalysts were synthesized for methane decomposition using a co-precipitation method, the incorporation of TiO_2 effectively reduced the formation of nickel aluminate (NiAl_2O_4) and the carbon deposition was greatly inhibited.⁴² In hydrodesulfurization reactions, TiO_2 - Al_2O_3 based catalysts also show unique advantages, TiO_2 promoted the formation of empty orbitals in multilayered MoS_2 , resulting in the strong sulfur adsorption capacity of the catalyst. The Ti^{3+} species formed by the partial reduction or sulfidation of TiO_2 can act as a promoter for the MoS_2 phase.^{43,44} A series of Mo/TiO_2 - Al_2O_3 catalysts were prepared by Segawa et al. via the chemical vapor deposition of TiCl_4 , and Mo/TiO_2 - Al_2O_3 exhibited higher activity than the $\text{Mo/Al}_2\text{O}_3$ or Mo/TiO_2 catalysts in the ultra-deep hydrodesulfurization reaction.⁴⁵⁻⁴⁷ This was attributed to the coverage of Al_2O_3 by TiO_2 layer, decreasing the interaction between Mo and the support and promoting the sulfidation of Mo species. In another report, by using TiO_2 - Al_2O_3 binary supports for the Ni/Mo -based catalysts, the hydrodesulfurization activity of the catalysts was improved due to the enhanced hydrogenation activity by the existence of TiO_2 .⁴⁸ In recent studies, highly ordered NiMo/TiO_2 - Al_2O_3 hydrodesulfurization catalysts were prepared via evaporation-induced self-assembly method.^{49,50} Their results demonstrated that the introduction of TiO_2 into the supports prevented the formation of strong Mo-O-Al linkages which promoted the formation of "Type II" Ni-Mo-S phase and enhanced the activity of the catalysts. Inspired by the promotion effect of TiO_2 , it can be envisaged that the

formation of spinel structures in adsorbents may be effectively inhibited by introducing TiO_2 into the $\text{Ni/ZnO-Al}_2\text{O}_3$ adsorbents. The incorporation of TiO_2 into Al_2O_3 will construct a TiO_2 protection layer between ZnO and Al_2O_3 , which would isolate the ZnO from Al_2O_3 . The inserted TiO_2 would competitively react with Al_2O_3 to form Ti-O-Al bonds, inhibiting the formation of Zn-O-Al bonds.

This work aims to propose a new method to inhibit the spinel formation in $\text{Ni/ZnO-Al}_2\text{O}_3$ based RADS adsorbents via TiO_2 addition. The TiO_2 modified Al_2O_3 support was synthesized by the wet impregnation method and used for the preparation of $\text{Ni/ZnO-Al}_2\text{O}_3$ based adsorbents via a heterogeneous-grinding method. The performance of the adsorbents was evaluated in the RADS reaction using a model fuel and compared with the adsorbents prepared without TiO_2 .

2. Results

2.1 Reaction Adsorption Desulfurization (RADS) Performance of Adsorbents

In order to eliminate the influence brought by reaction products (ZnS , NiS_x , etc.), we chose the fresh TiO_2 modified and unmodified adsorbents (supports) with a Zn/Al molar ratio of 1:1 to undergo the cyclic hydrothermal treatments, which can clearly reveal the promotion effect of TiO_2 addition. The adsorbents were denoted as 'Ti-a-b-c' and 'C-a-b-c', where 'Ti' represents TiO_2 modified, 'C' represents unmodified, 'a-b' indicates the molar ratio of Zn to Al , and 'c' indicates the cycles of the hydrothermal treatment. The 'S' was attached behind the name of adsorbents to present the corresponded supports. Figure 1 shows the sulfur adsorption breakthrough curves and the breakthrough sulfur capacities of the fresh adsorbents and the adsorbents after 3 cycles of hydrothermal treatment, respectively. As can be seen, the fresh unmodified adsorbent exhibited a better RADS activity and a higher sulfur capacity than the fresh TiO_2 modified adsorbent. After three cycles of hydrothermal treatment, the TiO_2

modified adsorbent exhibited a higher sulfur capacity than the unmodified one, indicating the higher stability of the former. The breakthrough sulfur capacity (at 10 ppm Sulfur) of the TiO₂ modified adsorbent decreased from 10.5 mg·g⁻¹ to 7.8 mg·g⁻¹ which is above 2-fold that of the unmodified adsorbent (3.8 mg·g⁻¹) after 3 cycles of hydrothermal treatment. The ZnO conversion revealing the ZnO transformation extent is another important indicator of the catalyst activity and stability. The ZnO conversion at the breakthrough point for the fresh TiO₂ modified adsorbent (7.04%) is slightly lower than that of the unmodified one (7.62%). Although both adsorbents exhibit a decrease in their ZnO conversion which was caused by the hydrothermal treatments, the TiO₂ modified one retained 74.1% of its ZnO conversion in the fresh state, while the unmodified one only maintained 31.4% of its fresh ZnO conversion. These results clearly indicated that the stability of the adsorbent could be significantly enhanced by modifying the Ni/ZnO-Al₂O₃ adsorbent with TiO₂.

2.2 Crystalline Structure

X-ray fluorescence (XRF) spectra results shown in Table S2 show that the bulk atomic molar ratio of the TiO₂ modified adsorbents (Zn: Ti: Al = 1.22: 0.18: 1.00) is close to the set ratio (Zn: Ti: Al=1.00: 0.15: 1.00), thus indicating that most of the introduced TiO₂ was kept in the bulk structure without significant loss during the preparation process. The PXRD patterns of the TiO₂ modified and unmodified adsorbents are shown in Figure 2. All fresh adsorbents contain hexagonal wurtzite (ZnO, JCPDS card No. 01-079-2205) and cubic NiO (JCPDS card No. 01-078-0429) phases, and there are no obvious characteristic reflections of TiO₂ phase in the TiO₂ modified adsorbents, indicating that the TiO₂ is highly dispersed. For the unmodified adsorbents, the intensities of characteristic reflections assignable to cubic gahnite (ZnAl₂O₄, JCPDS card No.00-001-1146, 2θ= 44.83°, 59.2° and 65.20°) raised with the increasing cycles of hydrothermal treatment. In contrast, the peak intensities of ZnAl₂O₄ in the TiO₂ modified adsorbents are much lower than those in the unmodified ones. To support the results revealing

the interactions between ZnO and Al₂O₃ leading to the stability enhancement by TiO₂ addition, the TiO₂ modified and unmodified adsorbents with Zn/Al molar ratios of 1:2 and 1:4 were tested by cyclic hydrothermal treatments (shown in Figure S2 and S3). The peak intensities of ZnAl₂O₄ raised with the increase of the Al₂O₃ amount which may be due to the higher dispersion of ZnO caused by the increase in Al₂O₃ content, promoting the interactions between ZnO and Al₂O₃. While the TiO₂ modified adsorbents still exhibited lower peak intensities for the ZnAl₂O₄ phase than the unmodified ones. These results directly prove that the addition of TiO₂ in the ZnO-Al₂O₃ based adsorbents could effectively impede the interaction between the sulfur acceptor (ZnO) and the support (Al₂O₃) to form the inactive ZnAl₂O₄ spinel, which partially explains the high activity and large sulfur capacity of the modified adsorbents after hydrothermal treatments.

UV-vis spectra of TiO₂ modified and unmodified supports are shown in Figure 3. The peaks at 280 nm and 314 nm could be attributed to the existence of ZnAl₂O₄.⁵¹ The peak at 320 nm is due to the O²⁻→Ti⁴⁺ charge transfer transition corresponding to the excitation of electrons from the valence band (having the O 2p character) to the conduction band (having the Ti 3d character), which is the characteristic of anatase phase.⁵² For the fresh supports, there are no discernable peaks assignable to ZnAl₂O₄. While after the hydrothermal treatments, the peak intensities corresponding to ZnAl₂O₄ in the unmodified supports increased with the hydrothermal treatment cycles. However, there are no discernable ZnAl₂O₄ peaks in the TiO₂ modified supports, evidencing the high stability of the TiO₂ modified samples which is consistent with the PXRD results.

2.3 Morphology and Textural Properties

Figure 4 and 5 show the SEM and EDS-mapping images of both TiO₂ modified and unmodified supports. In both supports, the ZnO particles were homogeneously dispersed on

the Al_2O_3 . For the TiO_2 modified support, the Ti species are also homogeneously dispersed on the Al_2O_3 . Considering there are no obvious peaks of titania in the PXRD patterns of TiO_2 modified adsorbents (shown in Figure 2), the introduced TiO_2 may be present as highly dispersed TiO_2 species and covered the alumina surfaces after calcination.⁵³

Figure 6 shows N_2 sorption isotherms of the unmodified and TiO_2 modified adsorbents with a Zn/Al molar ratio of 1: 1. All samples display typical type IV adsorption isotherms with an H-3 hysteresis loop, indicating the existence of a mesoporous structure.⁵⁴ The textural properties of the adsorbents are summarized in Table S3. For the fresh adsorbents, compared with the unmodified adsorbents, the TiO_2 modified one has a lower specific surface area which may be due to the partial blocking of the pores by TiO_2 , and this may also be a reason for the lower activity of fresh TiO_2 modified adsorbent in the RADS reaction (shown in Figure 1).⁵³ With increasing the cycles of hydrothermal treatment, the specific surface areas of both unmodified and TiO_2 modified adsorbents decreased, which may be due to the formation of spinel, sintering and collapse of pore structure. However, the addition of TiO_2 could inhibit the formation of ZnAl_2O_4 spinel and enhance the pore structure stability during hydrothermal treatments. The TiO_2 modified samples exhibit less reduction of the surface area. In comparison, the unmodified adsorbent lost 21% of its specific surface area after three cycles of hydrothermal treatment, while the specific surface area of the TiO_2 modified sample reduced by 17%. Increasing the Al_2O_3 amount in the adsorbents could increase the specific surface area and enhance the dispersion of ZnO and NiO (Figure S8 and Table S3). However, this will also promote the formation of spinel under the reaction/regeneration conditions, which imposed a deleterious effect on the stability and activity of adsorbents. Moreover, the stability enhancement brought by the introduced TiO_2 is more pronounced.

2.4 State of TiO₂ and Surface Acidity

The unmodified (C-1-1-0-S and C-1-1-3-S) and TiO₂ modified (Ti-1-1-0-S and Ti-1-1-3-S) supports were characterized with Raman spectroscopy to detect the state of Ti in the TiO₂ modified supports. Both the TiO₂ modified and unmodified supports have the characteristic peaks of ZnO located at 99, 333 and 437 cm⁻¹ (Figure 7).⁵⁵ Besides, there is a peak at 146 cm⁻¹ that appears in the Raman spectrum of the TiO₂ modified support, which reveals the presence of anatase phase.⁵⁶ As shown by SEM and EDS-mapping (shown in Figure 5), the TiO₂ was highly dispersed on the Al₂O₃ surface; the TiO₂ as anatase formed protection layer, which could inhibit the formation of ZnAl₂O₄ spinel phase by preventing the interaction between ZnO and Al₂O₃ during RADS reaction and regeneration processes.

FT-IR spectra of unmodified and TiO₂ modified adsorbents are shown in Figure 8a and 8b. The peaks at 940 and 1380 cm⁻¹ are attributed to the Zn-O bond vibration.^{57,58} The weak shoulder at 1100 cm⁻¹ corresponds to Al-O vibration typical for γ -alumina, which is confirmed by the presence of the peak at 1630 cm⁻¹.^{59,60} The broad band at 3200-3700 cm⁻¹ is the stretching vibration band of -OH bonded to Al³⁺. No band assigned to Ti-O-Al bond at 1128 cm⁻¹ is found in the spectra of TiO₂ modified adsorbents, suggesting no strong interactions between TiO₂ and γ -Al₂O₃.⁶¹ The FT-IR results combined with PXRD (Figure 2) and XRF (Table S2) suggest that the TiO₂ is evenly spread over the γ -Al₂O₃ and inhibited the interactions between ZnO and γ -Al₂O₃.

The Py-IR spectra of unmodified and TiO₂ modified adsorbents are depicted in Figure 8c and 8d. The Lewis acid sites are identified by the presence of the bands at 1450 (ν_{19b}), 1490 (ν_{19a}) and 1610 (ν_{18a}) cm⁻¹, while the peak at 1578 cm⁻¹ is attributed to the interaction between α -pyridine and -OH on the adsorbent surface.⁶² The amount of Lewis acid sites for the unmodified and TiO₂ modified adsorbents after cyclic hydrothermal treatments are

summarized in Table S4. For the fresh adsorbents, the Lewis acid amount of unmodified adsorbent was higher than that of the TiO₂ modified one. This may be due to the formation of the anatase layer which partly blocked the pores and covered the defects on the surfaces. With increasing the cycles of hydrothermal treatment, the Lewis acid amounts of both unmodified and TiO₂ modified adsorbents changed. For the unmodified adsorbent, the amount of Lewis acid sites decreased by 35.48% after the first cycle of the hydrothermal treatment and almost remained the same in the following cycles. This may be caused by the pore structure destruction or sintering and the formation of ZnAl₂O₄. However, the TiO₂ modified adsorbent exhibited better hydrothermal stability; the amount of Lewis acid sites decreased by 23.81% after the first cycle of hydrothermal treatment. It is quite interesting to note that, the amount of Lewis acid sites started to raise with the increase of the hydrothermal treatment cycles. The Lewis acid amount recovered 14.29% in cycle 2, and dramatically increased to 3.1 mmol·g⁻¹ which is 32.26% higher than that of the fresh TiO₂ modified adsorbent in cycle 3. This may be attributed to the formation of new acid sites resulting from the structural rearrangement during the hydrothermal treatments. Since the Lewis acid sites are beneficial for the adsorption of thiophene bearing lone pair electrons,⁶³ the higher concentration of Lewis acid sites in TiO₂ modified sample after 3 cycles of hydrothermal treatment may be partially responsible for the improved RADS performance as compared to the unmodified one.²³

3. Discussion

The highly dispersed TiO₂ on the γ -Al₂O₃ was verified based on the results shown above (see Figure 2 and 5, Table S2) which is in line with the study of Zhang et al.⁶¹ In addition, the Raman spectra (Figure 7) confirmed the existence of anatase TiO₂ on the support surface with good stability; no formation of new compounds after three cycles of hydrothermal treatment was observed. Based on the above results, a schematic illustration explaining the role of TiO₂ in inhibiting the ZnAl₂O₄ formation is presented in Figure 9. As both the γ -Al₂O₃ (the pseudo-

boehmite was transformed to γ -Al₂O₃ after calcination) and ZnAl₂O₄ have a similar space group (Fd-3m), it is easy for the Zn²⁺ (in adjacent ZnO) to diffuse into the tetrahedral sites of γ -Al₂O₃ during the RADS reaction and regeneration process. A thin layer of TiO₂ covered on the γ -Al₂O₃ surface would isolate ZnO from the direct contact with γ -Al₂O₃, and then weaken the interaction between Zn²⁺ and Al³⁺ to prevent the formation of ZnAl₂O₄ structure. Along with hindering the formation of the ZnAl₂O₄, the TiO₂ protection layer could also be beneficial for the maintenance of the pore structure of the γ -Al₂O₃. The destruction of pore structures during high-temperature reaction-regeneration cycles caused by the agglomeration or Al-O-Al breakage and sintering of ZnO was a common problem, which resulted in the decrease of the specific surface area of adsorbents.^{64,65} This problem was also observed in the unmodified adsorbents in this work (the specific surface area decreased by 20.96% after 3 cycles of hydrothermal treatment). The TiO₂ modified adsorbent exhibited higher pore structure stability with the protection from TiO₂ on the surface even though the pore structure was partially blocked by the TiO₂. The difference in pore structure stability was more evident with the increase of the Al content. As shown in Table S3, the surface area of sample C-1-4-3 decreased by 46.93%, while for sample Ti-1-4-3 decreased only by 14.02% after 3 cycles of hydrothermal treatment. This may be due to the TiO₂ coverage on the γ -Al₂O₃ surface, hindering the collapse of pore structures and retarding the growth or reconstruction of γ -Al₂O₃ crystals that can result in the formation of new Al-O-Al bonds. Moreover, all spectroscopy results indicated no formation of new bonds or phases during the cyclic hydrothermal treatments, implying that the TiO₂ protection layer could not only effectively prevent the formation of ZnAl₂O₄ but also maintain stable during the reaction and regeneration processes. Thus, it will not cause the formation of Ti-O-Zn bonds and adverse effect on the activity of ZnO. Besides, although there is no evidence of Ti-O-Al formation during the reaction and hydrothermal treatments, the possibility for its formation can't be completely excluded.^{47,66} There are a certain amount of defects on the surface of γ -Al₂O₃, which are associated with the

exposed O vacancies and unsaturated coordinated Al^{3+} sites. As has been shown in Figure 7, the peak intensity of the anatase phase became more intense with the increase of hydrothermal treatment cycles, indicating the growth of anatase crystals. As a result, the possibility of Ti-O-Al formation is increasing during the growth or reconstruction of the TiO_2 layer as the coordination unsaturated (CUS) Al^{3+} sites on the $\gamma\text{-Al}_2\text{O}_3$ surface are close to the TiO_2 layer (see Figure 9). The formation of Ti-O-Al could be in competition to the formation of Zn-O-Al (or Al-O-Al) by occupying the unsaturated coordinated Al^{3+} sites, which could enhance the stability of the adsorbent.⁶⁷ The high structural stability of the TiO_2 modified adsorbent ensured that the ZnO can react with sulfur by preventing the formation of ZnAl_2O_4 , thus achieving the superior activity of ZnO after the hydrothermal treatment cycles as compared with the unmodified one.

The existence of Lewis acid sites could provide empty orbitals on the adsorbent surfaces which could promote the adsorption of sulfur (bearing lone pair electrons) in the organic sulfur molecules (such as thiophene) and then facilitate the reaction. The Lewis acid sites on the $\gamma\text{-Al}_2\text{O}_3$ surface originate mainly from the CUS Al^{3+} sites caused by the -OH removal and phase transformations during the calcination process.^{59,68,69} In the unmodified adsorbent, the Lewis acid amount decreased by 35.48% after the first cycle of hydrothermal treatment. Two main reasons for this result are suggested: (1) the interaction between Zn^{2+} and surface CUS Al^{3+} sites generating the ZnAl_2O_4 spinel phase (see results presented in Figure 2 and 3); as a result, the empty orbital of the CUS Al^{3+} was filled, causing the loss of Lewis acidity; (2) the agglomeration (see in Table S3) and reconstruction of the support surface led to the formation of new Al-O-Al bonds and the loss of CUS Al^{3+} sites from the surface. However, the Lewis acid amount recovered slightly (3.22%) after three cycles of hydrothermal treatment, which may be due to the dissociation of the $\gamma\text{-Al}_2\text{O}_3$ surface structure under the high-temperature steaming environment. During the hydrothermal treatments, a dissolution-recrystallization

process would occur on the surface of $\gamma\text{-Al}_2\text{O}_3$. The H_2O would dissociate and interact with the surface Al^{3+} by inserting H^+ into the Al-O-Al to form Al-OH that can result in the formation of defects and CUS Al^{3+} after dehydration.⁷⁰ This process could partially recover the acidity of the adsorbent, but could not reverse the decreasing trend of the Lewis acid amount. For TiO_2 modified adsorbent, the initial Lewis acid amount ($2.1 \text{ mmol}\cdot\text{g}^{-1}$) was lower than that of the fresh unmodified one ($3.1 \text{ mmol}\cdot\text{g}^{-1}$), but the TiO_2 modified adsorbent showed a lower decrease of Lewis acid amount (-23.81%) than the unmodified adsorbent (-35.48%) after the first hydrothermal treatment cycle. The TiO_2 protection layer impeded the formation of Zn-O-Al bonds which could maintain the Lewis acid sites on the surface. However, the coverage of the TiO_2 layer also blocked parts of the pores and restrained the exposure of the Lewis acid sites. Moreover, the underlying formation of Ti-O-Al would further decrease the total amount of Lewis acid sites on the surface. With increasing the hydrothermal treatment cycles, the new acid sites generated by TiO_2 offset the loss of Lewis acidity caused by TiO_2 coverage and Ti-O-Al formation which was not detected. As a result, the Lewis acid amount in the sample after three cycles of hydrothermal treatment was even 32.26% higher than that in the freshly TiO_2 modified adsorbent. This is because the hydroxyl ions and H^+ formed during hydrothermal treatments would not only affect the $\gamma\text{-Al}_2\text{O}_3$ but also the TiO_2 . As been recognized previously, the hydrothermal treatment would also promote the intergrowth (crystallization) or reconstruction of the TiO_2 (anatase) layers,⁷¹ similar to what would happen to $\gamma\text{-Al}_2\text{O}_3$, the H^+ may also break the Ti-O-Ti(Al) and the hydroxyl ions may coordinate with the unsaturated Ti cations. As a consequence, the growth process will inevitably produce new or break Ti-O-Ti (Al) bonds and expose coordinatively unsaturated Ti cations (5 or 4 coordinated) with the dissociation of hydroxyl ions or Ti-O-Ti (Al) cleavage,⁶⁷ the unsaturated Ti cations would be the new Lewis acid sites.^{53,72} Besides, the flexible chemical valence state of Ti would also be helpful for producing more Lewis acid sites on the surface. The H_2 treatments in reduction and reaction processes would reduce the surface of TiO_2 and

produce $\text{Ti}^{(4-\delta)}$. Afterward, the regeneration process (calcination) would oxidize the Ti^{4+} to a higher state ($\text{Ti}^{(4+\alpha)}$); both Ti cations exhibit Lewis acidity which would be helpful for the adsorption of organic sulfur compound.^{53,73}

4. Conclusions

In this work, a series of TiO_2 modified Al_2O_3 supports were synthesized by the wet impregnation method and used in the preparation of $\text{Ni/ZnO-Al}_2\text{O}_3$ adsorbents via a heterogeneous-grinding method. Both the TiO_2 modified and unmodified adsorbents were evaluated in the RADS reaction using a model fuel with a high sulfur concentration (500 ppm).

By incorporating TiO_2 in the $\text{ZnO-Al}_2\text{O}_3$ support to form a thin anatase protection layer, the formation of the ZnAl_2O_4 spinel phase was effectively inhibited which significantly improved the stability of the final adsorbents. By generating new Lewis acid sites, the TiO_2 modified adsorbent maintained a good adsorption ability for organic sulfur compounds in feeds, which enhanced the catalytic activity of the adsorbent. After 3 cycles of hydrothermal treatments, the breakthrough sulfur capacity (at 10 ppm Sulfur) of the TiO_2 modified adsorbent kept at $7.8 \text{ mg}\cdot\text{g}^{-1}$ which is two times higher than that for the unmodified adsorbent ($3.8 \text{ mg}\cdot\text{g}^{-1}$), even though the initial sulfur capacity of the fresh TiO_2 modified one is slightly lower than that in the unmodified one.

Hence, to modify the $\text{ZnO-Al}_2\text{O}_3$ supports by the TiO_2 protection layer is a viable strategy to inhibit the formation of inactive spinel structures and improve the stability of the RADS adsorbent.

Supporting Information

Supporting Information is available from the Wiley Online Library or from the author.

Acknowledgments

This work was financially supported by the National Key Research and Development Program of China (2017YFB0306600), the National Key Technologies R & D Program of China (2018YFE0118200), Natural Science Foundation of China (51601223, 21206195, U1510109), the Fundamental Research Funds for the Central Universities (17CX05018, 17CX02056, 14CX02050A, 14CX02123A), Shandong Provincial Natural Science Foundation (ZR2017MB003) and State Key Laboratory of Heavy Oil Processing Fund (SKLZZ-2017008).

Received: ((will be filled in by the editorial staff))

Revised: ((will be filled in by the editorial staff))

Published online: ((will be filled in by the editorial staff))

References

1. Zhang K, Wen Z. Review and challenges of policies of environmental protection and sustainable development in China. *Journal of environmental management*. 2008;88(4):1249-1261.
2. Hunter KA, Liss PS, Surapipith V, et al. Impacts of anthropogenic SO_x, NO_x and NH₃ on acidification of coastal waters and shipping lanes. *Geophysical Research Letters*. 2011;38(13).
3. Munawer ME. Human health and environmental impacts of coal combustion and post-combustion wastes. *Journal of Sustainable Mining*. 2018;17(2):87-96.
4. Heck RM, Farrauto RJ, Gulati ST. *Catalytic air pollution control: commercial technology*. John Wiley & Sons; 2016.
5. Breyse M, Djega-Mariadassou G, Pessayre S, et al. Deep desulfurization: reactions, catalysts and technological challenges. *Catalysis Today*. 2003;84(3-4):129-138.
6. Shen Y, Li P, Xu X, Liu H. Selective adsorption for removing sulfur: a potential ultra-deep desulfurization approach of jet fuels. *RSC Advances*. 2012;2(5):1700-1711.
7. Kim J, Ma X, Zhou A, Song C. Ultra-deep desulfurization and denitrogenation of diesel fuel by selective adsorption over three different adsorbents: a study on adsorptive selectivity and mechanism. *Catalysis Today*. 2006;111(1-2):74-83.

8. Song C. An overview of new approaches to deep desulfurization for ultra-clean gasoline, diesel fuel and jet fuel. *Catalysis today*. 2003;86(1-4):211-263.
9. Ma X, Sun L, Song C. A new approach to deep desulfurization of gasoline, diesel fuel and jet fuel by selective adsorption for ultra-clean fuels and for fuel cell applications. *Catalysis today*. 2002;77(1-2):107-116.
10. Bielecki J. Energy security: is the wolf at the door? *The quarterly review of economics and finance*. 2002;42(2):235-250.
11. Song C. New approaches to deep desulfurization for ultra-clean gasoline and diesel fuels: an overview. *Prepr Pap Am Chem Soc Div Fuel Chem*. 2002;47(2):438-444.
12. Skea J. What drives clean fuel technology? *Proceedings of the Institution of Mechanical Engineers, Part A: Journal of Power and Energy*. 1997;211(1):1-10.
13. Phillips C. S-Zorb Sulfur Removal Technology. Paper presented at: World Fuels Conference, Brüssel, Belgien 2001.
14. Sharma M, Vyas RK, Singh K. A review on reactive adsorption for potential environmental applications. *Adsorption*. 2013;19(1):161-188.
15. Ma X, Sprague M, Song C. Deep desulfurization of gasoline by selective adsorption over nickel-based adsorbent for fuel cell applications. *Industrial & Engineering Chemistry Research*. 2005;44(15):5768-5775.
16. Gupta M, He J, Nguyen T, et al. Nanowire catalysts for ultra-deep hydro-desulfurization and aromatic hydrogenation. *Applied Catalysis B: Environmental*. 2016;180:246-254.
17. Wang T, Wang X, Gao Y, et al. Reactive adsorption desulfurization coupling aromatization on Ni/ZnO-Zn₆Al₂O₉ prepared by Zn_xAl_y(OH)₂(CO₃)_z·xH₂O precursor for FCC gasoline. *Journal of energy chemistry*. 2015;24(4):503-511.
18. Huang L, Wang G, Qin Z, et al. A sulfur K-edge XANES study on the transfer of sulfur species in the reactive adsorption desulfurization of diesel oil over Ni/ZnO. *Catalysis Communications*. 2010;11(7):592-596.

19. Babich IV, Moulijn JA. Science and technology of novel processes for deep desulfurization of oil refinery streams: a review. *Fuel*. 2003;82(6):607-631.
20. Bezverkhyy I, Gadacz G, Bellat JP. Interaction of Ni/SiO₂ with thiophene. *Materials Chemistry and Physics*. 2009;114(2):897-901.
21. Bezverkhyy I, Ryzhikov A, Gadacz G, Bellat JP. Kinetics of thiophene reactive adsorption on Ni/SiO₂ and Ni/ZnO. *Catalysis Today*. 2008;130(130):199-205.
22. Ryzhikov A, Bezverkhyy I, Bellat JP. Reactive adsorption of thiophene on Ni/ZnO: Role of hydrogen pretreatment and nature of the rate determining step. *Applied Catalysis B: Environmental*. 2008;84(3-4):766-772.
23. Meng X, Huang H, Weng H, Shi L. Ni/ZnO-based adsorbents supported on Al₂O₃, SiO₂, TiO₂, ZrO₂: a comparison for desulfurization of model gasoline by reactive adsorption. *Bulletin of the Korean Chemical Society*. 2012;33(10):3213-3217.
24. Dehghan R, Anbia M. Zeolites for adsorptive desulfurization from fuels: A review. *Fuel Processing Technology*. 2017;167:99-116.
25. Sasaoka E, Sada N, Manabe A, Uddin MA, Sakata Y. Modification of ZnO–TiO₂ high-temperature desulfurization sorbent by ZrO₂ addition. *Industrial & engineering chemistry research*. 1999;38(3):958-963.
26. Wen Y, Wang G, Wang Q, Xu C, Gao J. Regeneration characteristics and kinetics of Ni/ZnO–SiO₂–Al₂O₃ adsorbent for reactive adsorption desulfurization. *Industrial & Engineering Chemistry Research*. 2012;51(10):3939-3950.
27. Wang G, Wen Y, Fan J, Xu C, Gao J. Reactive characteristics and adsorption heat of Ni/ZnO–SiO₂–Al₂O₃ adsorbent by reactive adsorption desulfurization. *Industrial & Engineering Chemistry Research*. 2011;50(22):12449-12459.
28. Fan J, Wang G, Sun Y, et al. Research on reactive adsorption desulfurization over Ni/ZnO–SiO₂–Al₂O₃ adsorbent in a fixed-fluidized bed reactor. *Industrial & Engineering Chemistry Research*. 2010;49(18):8450-8460.

29. Ullah R, Bai P, Wu P, et al. Superior performance of freeze-dried Ni/ZnO-Al₂O₃ adsorbent in the ultra-deep desulfurization of high sulfur model gasoline. *Fuel Processing Technology*. 2017;156:505-514.
30. Ullah R, Zhang Z, Bai P, et al. One-pot cation–anion double hydrolysis derived Ni/ZnO–Al₂O₃ adsorbent for reactive adsorption desulfurization. *Industrial & Engineering Chemistry Research*. 2016;55(13):3751-3758.
31. Ullah R, Bai P, Wu P, et al. Comparison of the reactive adsorption desulfurization performance of Ni/ZnO–Al₂O₃ adsorbents prepared by different methods. *Energy & Fuels*. 2016;30(4):2874-2881.
32. Xu G, Diao Y, Zou K, Zhang Z. Cause analysis of sorbent deactivation in S Zorb unit for gasoline desulfurization. *Petroleum Processing and Petrochemicals*. 2011;12.
33. Meng X, Huang H, Shi L. Reactive mechanism and regeneration performance of NiZnO/Al₂O₃-diatomite adsorbent by reactive adsorption desulfurization. *Industrial & Engineering Chemistry Research*. 2013;52(18):6092-6100.
34. Gil A, Diaz A, Montes M. Passivation and reactivation of nickel catalysts. *Journal of the Chemical Society, Faraday Transactions*. 1991;87(5):791-795.
35. Zou K, Lin W, Tian H, Xu G, Wang L, Xu H. Study on Zn₂SiO₄ formation kinetics and activity stability of desulfurization sorbent. *China Pet Process PE*. 2015;17:6-15.
36. Xu G, Diao Y, Zou K, Zhang Z. Cause analysis of sorbent deactivation in S-Zorb unit for gasoline desulfurization. *Pet Process Petrochem*. 2011;42(12):1-6.
37. Lyu Y, Sun Z, Xin Y, Liu Y, Wang C, Liu X. Reactivation of spent S-Zorb adsorbents for gasoline desulfurization. *Chemical Engineering Journal*. 2019;374:1109-1117.
38. Reddy BM, Ganesh I, Chowdhury B. Design of stable and reactive vanadium oxide catalysts supported on binary oxides. *Catalysis today*. 1999;49(1-3):115-121.
39. Hu S, Chen Y. Partial hydrogenation of benzene to cyclohexene on ruthenium catalysts supported on La₂O₃–ZnO binary oxides. *Industrial & engineering chemistry research*.

1997;36(12):5153-5159.

40. Kaneko E, Pulcinelli SH, Da Silva VT, Santilli CV. Sol-gel synthesis of titania-alumina catalyst supports. *Applied Catalysis A: General*. 2002;235(1-2):71-78.

41. Kainthla I, Babu GVR, Bhanushali JT, Rao KSR, Nagaraja BM. Development of stable $\text{MoO}_3/\text{TiO}_2\text{-Al}_2\text{O}_3$ catalyst for oxidative dehydrogenation of ethylbenzene to styrene using CO_2 as soft oxidant. *Journal of CO2 Utilization*. 2017;18:309-317.

42. Awadallah AE, Mostafa MS, Aboul-Enein AA, Hanafi SA. Hydrogen production via methane decomposition over $\text{Al}_2\text{O}_3\text{-TiO}_2$ binary oxides supported Ni catalysts: Effect of Ti content on the catalytic efficiency. *Fuel*. 2014;129:68-77.

43. Coulier L, Van Veen J, Niemantsverdriet J. TiO_2 -supported Mo model catalysts: Ti as promoter for thiophene HDS? *Catalysis letters*. 2002;79(1-4):149-155.

44. Okamoto Y, Maezawa A, Imanaka T. Active sites of molybdenum sulfide catalysts supported on Al_2O_3 and TiO_2 for hydrodesulfurization and hydrogenation. *Journal of Catalysis*. 1989;120(1):29-45.

45. Yoshinaka S, Segawa K. Hydrodesulfurization of dibenzothiophenes over molybdenum catalyst supported on $\text{TiO}_2\text{-Al}_2\text{O}_3$. *Catalysis Today*. 1998;45(1-4):293-298.

46. Saih Y, Segawa K. Tailoring of alumina surfaces as supports for NiMo sulfide catalysts in the ultra deep hydrodesulfurization of gas oil: case study of TiO_2 -coated alumina prepared by chemical vapor deposition technique. *Catalysis today*. 2003;86(1-4):61-72.

47. Saih Y, Nagata M, Funamoto T, Masuyama Y, Segawa K. Ultra deep hydrodesulfurization of dibenzothiophene derivatives over $\text{NiMo}/\text{TiO}_2\text{-Al}_2\text{O}_3$ catalysts. *Applied Catalysis A: General*. 2005;295(1):11-22.

48. Olguin E, Vrinat M, Ceden L, Ramirez J, Borque M, Lopez-Agudo A. The use of $\text{TiO}_2\text{-Al}_2\text{O}_3$ binary oxides as supports for Mo-based catalysts in hydrodesulfurization of thiophene and dibenzothiophene. *Applied Catalysis A: General*. 1997;165(1-2):1-13.

49. Zhang P, Mu F, Zhou Y, et al. Synthesis of highly ordered $\text{TiO}_2\text{-Al}_2\text{O}_3$ and catalytic

performance of its supported NiMo for HDS of 4, 6-dimethyldibenzothiophene. *Catalysis Today*. 2020.

50. Zhou W, Yang L, Liu L, et al. Synthesis of novel NiMo catalysts supported on highly ordered TiO₂-Al₂O₃ composites and their superior catalytic performance for 4, 6-dimethyldibenzothiophene hydrodesulfurization. *Applied Catalysis B: Environmental*. 2020;268:118428.

51. Sampath SK, Cordaro JF. Optical properties of zinc aluminate, zinc gallate, and zinc aluminogallate spinels. *Journal of the American Ceramic Society*. 2010;81(3):649-654.

52. Damyanova S, Spojakina A, Jiratova K. Effect of mixed titania-alumina supports on the phase composition of NiMo/TiO₂-Al₂O₃ catalysts. 1995;125(2):257-269.

53. Ramírez J, Rayo P, Gutiérrez-Alejandre A, Ancheyta J, Rana MS. Analysis of the hydrotreatment of Maya heavy crude with NiMo catalysts supported on TiO₂-Al₂O₃ binary oxides: Effect of the incorporation method of Ti. *Catalysis Today*. 2005;109(1):54-60.

54. Sotomayor FJ, Cychosz KA, Thommes M. Characterization of micro/mesoporous materials by physisorption: Concepts and case studies. *Acc Mater Surf Res*. 2018;3(2):34-50.

55. Montenegro DN, Hortelano V, Martínez O, et al. Non-radiative recombination centres in catalyst-free ZnO nanorods grown by atmospheric-metal organic chemical vapour deposition. *Journal of Physics D Applied Physics*. 2013;46(23):235302.

56. Dirnstorfer I, Mähne H, Mikolajick T, Knaut M, Albert M, Dubnack K. Atomic layer deposition of anatase TiO₂ on porous electrodes for dye-sensitized solar cells. *Journal of Vacuum Science & Technology A Vacuum Surfaces & Films*. 2012;31(1):5.

57. Sharma R, Alam F, Sharma AK, Dutta V, Dhawan SK. ZnO anchored graphene hydrophobic nanocomposite-based bulk heterojunction solar cells showing enhanced short-circuit current. *Journal of Materials Chemistry C*. 2014;2(38):8142-8151.

58. Devi BSR, Raveendran R, Vaidyan AV. Synthesis and characterization of Mn²⁺-doped ZnS nanoparticles. *Pramana*. 2007;68(4):679-687.

59. Toledo RR, Santoyo VR, Sánchez DM, Rosales MM. Effect of aluminum precursor on physicochemical properties of Al₂O₃ by hydrolysis/precipitation method. *Nova Scientia*. 2018;10(20):83-99.
60. Zhang C, Liu Z, Chen L, Dong Y. Influence of pH, humic acid, ionic strength, foreign ions, and temperature on ⁶⁰Co (II) sorption onto γ -Al₂O₃. *Journal of Radioanalytical and Nuclear Chemistry*. 2012;292(1):411-419.
61. Bing J, Hu C, Zhang L. Enhanced mineralization of pharmaceuticals by surface oxidation over mesoporous γ -Ti-Al₂O₃ suspension with ozone. *Applied Catalysis B: Environmental*. 2017;202:118-126.
62. Andonova SM, Şentürk GS, Kayhan E, Ozensoy E. Nature of the Ti–Ba interactions on the BaO/TiO₂/Al₂O₃ NO_x storage system. *Journal of Physical Chemistry C*. 2009;113(25):11014-11026.
63. Larrubia MA, Gutiérrez-Alejandre Ad, Ramírez J, Busca G. A FT-IR study of the adsorption of indole, carbazole, benzothiophene, dibenzothiophene and 4, 6-dibenzothiophene over solid adsorbents and catalysts. *Applied Catalysis A: General*. 2002;224(1-2):167-178.
64. Nair J, Nair P, Mizukami F, et al. Pore structure evolution of lanthana–alumina systems prepared through coprecipitation. *Journal of the American Ceramic Society*. 2000;83(8):1942-1946.
65. Choi J, Kim J, Yoo K, Lee T. Synthesis of mesoporous TiO₂/ γ -Al₂O₃ composite granules with different sol composition and calcination temperature. *Powder Technology*. 2008;181(1):83-88.
66. Segawa K, Takahashi K, Satoh S. Development of new catalysts for deep hydrodesulfurization of gas oil. *Catalysis Today*. 2000;63(2-4):123-131.
67. Ahmed M, Abdel-Messih M. Structural and nano-composite features of TiO₂–Al₂O₃ powders prepared by sol–gel method. *Journal of Alloys and Compounds*. 2011;509(5):2154-2159.

68. Morterra C, Bolis V, Magnacca G. IR spectroscopic and microcalorimetric characterization of Lewis acid sites on (transition phase) Al₂O₃ using adsorbed CO. *Langmuir : the ACS journal of surfaces and colloids*. 1994;10(6):1812-1824.
69. Zaki MI, Hasan MA, Al-Sagheer FA, Pasupulety L. In situ FTIR spectra of pyridine adsorbed on SiO₂-Al₂O₃, TiO₂, ZrO₂ and CeO₂: general considerations for the identification of acid sites on surfaces of finely divided metal oxides. *Colloids and Surfaces A: Physicochemical and Engineering Aspects*. 2001;190(3):261-274.
70. Li H, Li M, Nie H. Tailoring the surface characteristic of alumina for preparation of highly active NiMo/Al₂O₃ hydrodesulfurization catalyst. *Microporous and mesoporous materials*. 2014;188:30-36.
71. Hsiang HI, Lin SC. Effects of aging on the phase transformation and sintering properties of TiO₂ gels. *Materials Science and Engineering: A*. 2004;380(1-2):67-72.
72. Lee M, Seo Y, Shin HS, Jo C, Ryoo R. Anatase TiO₂ nanosheets with surface acid sites for Friedel-Crafts alkylation. *Microporous and Mesoporous Materials*. 2016;222:185-191.
73. Bhattacharyya K, Danon A, K. Vijayan B, Gray KA, Stair PC, Weitz E. Role of the surface lewis acid and base sites in the adsorption of CO₂ on titania nanotubes and platinumized titania nanotubes: An in situ FT-IR study. *The Journal of Physical Chemistry C*. 2013;117(24):12661-12678.

Figure 1. RADS breakthrough (10 ppm) (a) curves and (b) sulfur capacities of TiO₂ modified and unmodified adsorbents with a Zn/Al molar ratio of 1:1.

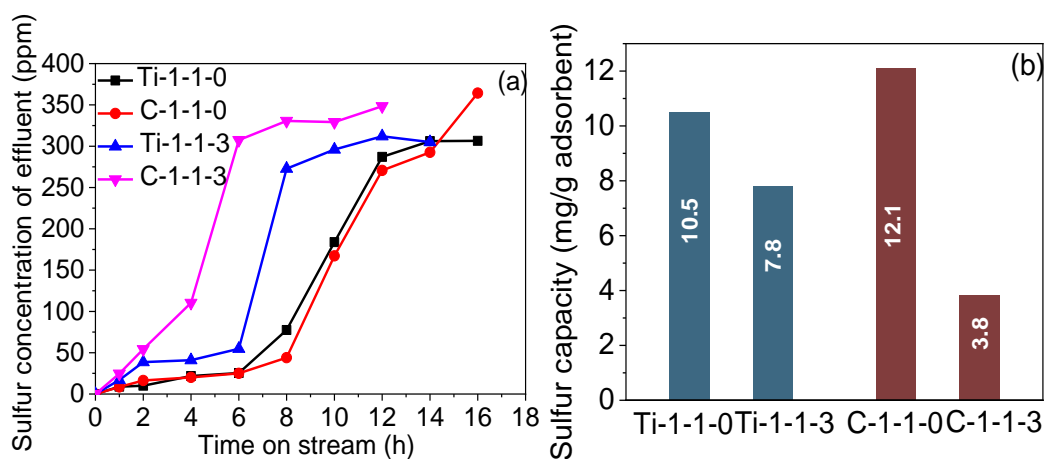


Figure 2. Powder X-ray diffraction (PXRD) patterns of (a) TiO₂ modified and (b) unmodified adsorbents with Zn/Al molar ratio of 1:1.

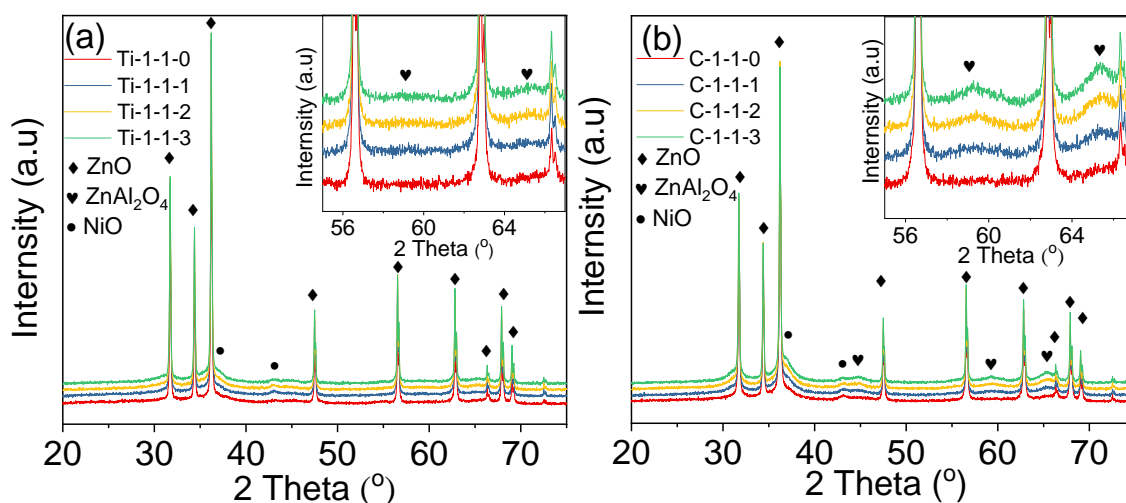


Figure 3. UV-visible spectra of TiO₂ modified and unmodified supports with a Zn/Al molar ratio of 1:1.

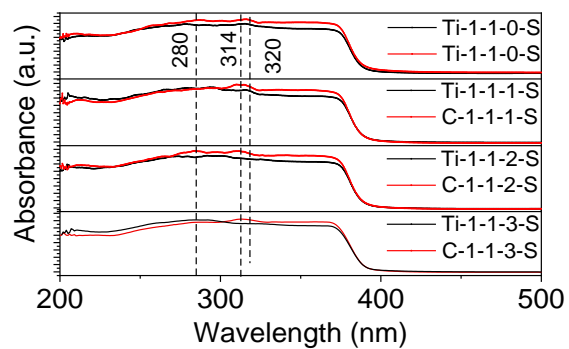


Figure 4. SEM and EDS-mapping images of unmodified supports.

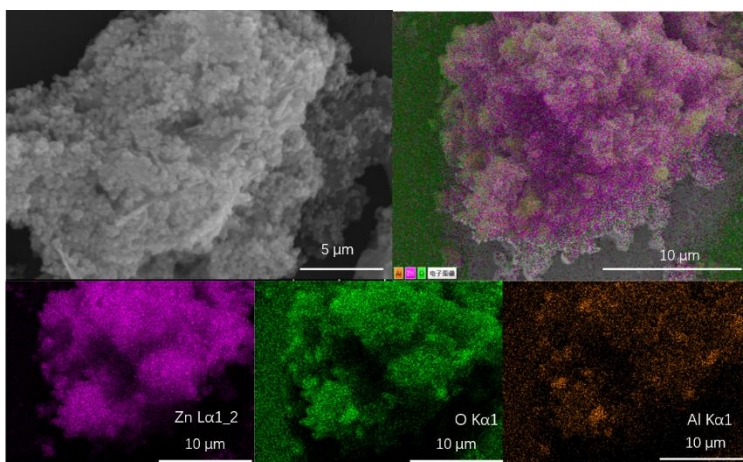


Figure 5. SEM and EDS-mapping images of TiO₂ modified supports.

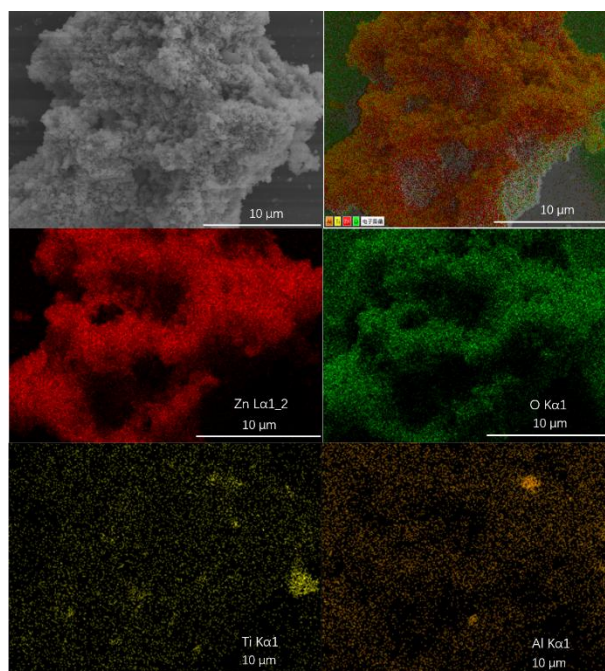


Figure 6. N₂ adsorption-desorption isotherms and PSD curves of (a) and (b) unmodified adsorbents, respectively and (c) and (d) TiO₂ modified adsorbents, respectively with a Zn/Al molar ratio of 1:1.

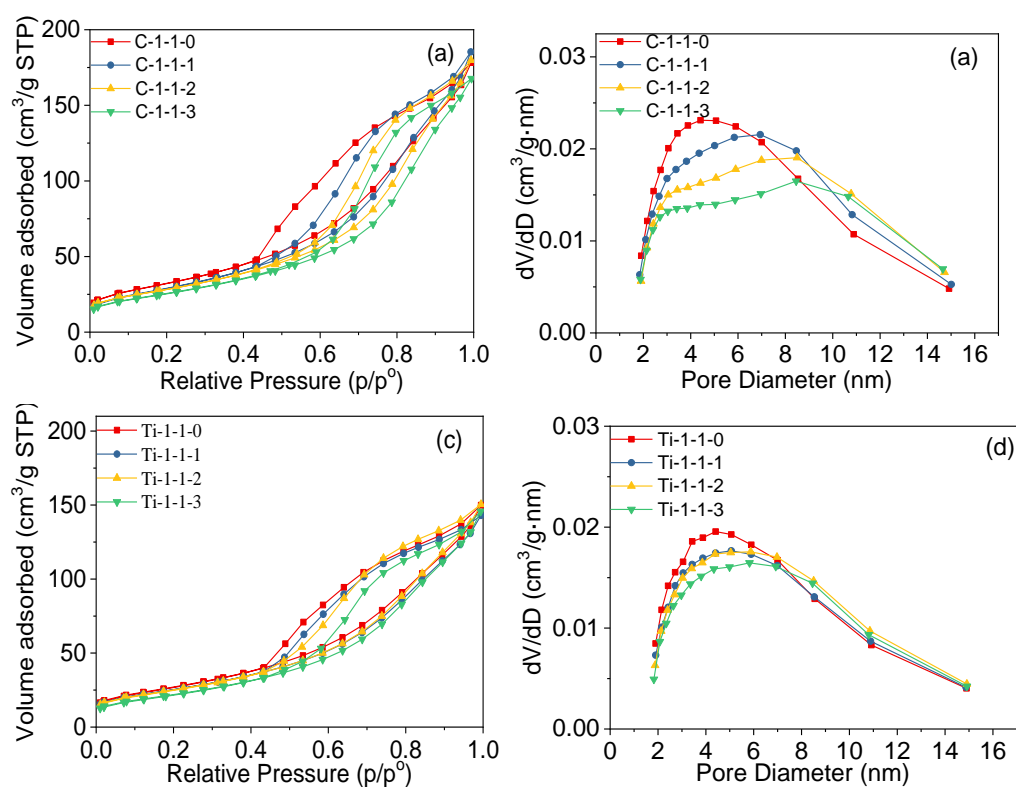


Figure 7. Raman spectra of TiO₂ modified and unmodified supports with a Zn/Al molar ratio of 1:1.

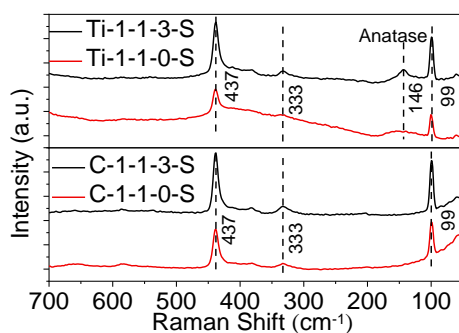


Figure 8. FT-IR spectra of (a) unmodified adsorbents, (b) TiO₂ modified adsorbents and Py-IR spectra of (c) unmodified adsorbents, (d) TiO₂ modified adsorbents with a Zn/Al molar ratio of 1:1.

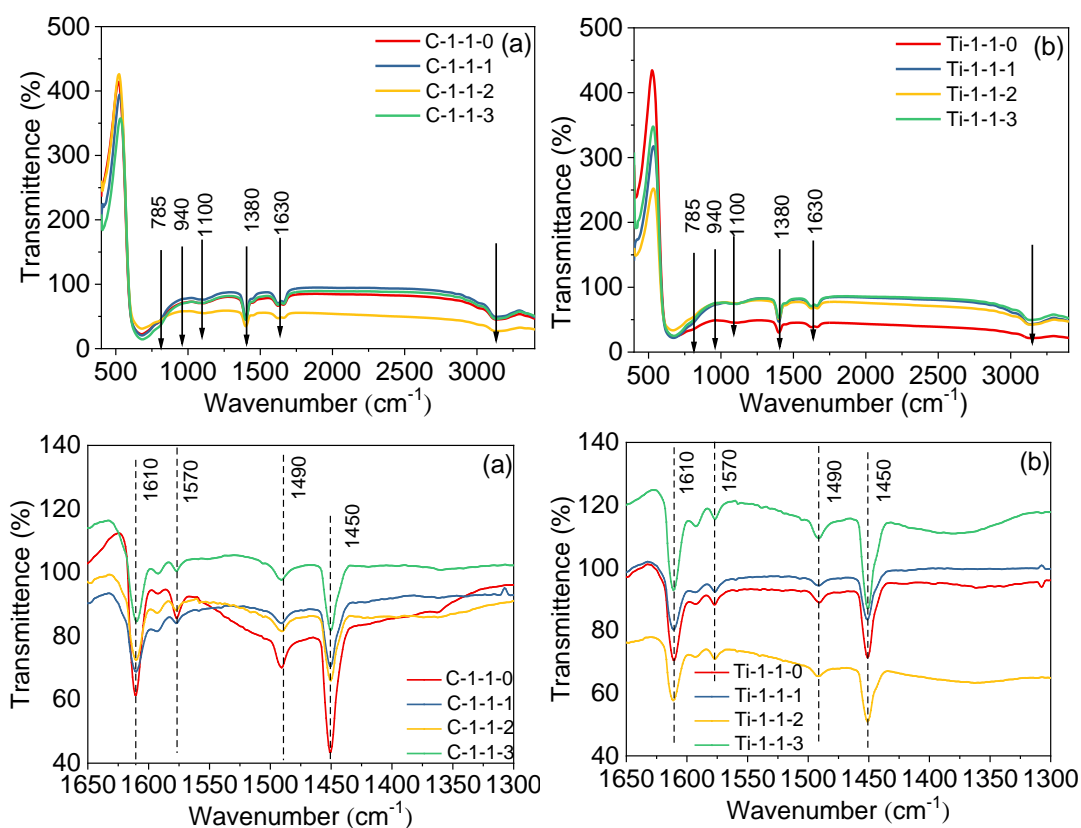


Figure 9. Graphical representation of TiO₂ layer inhibiting the formation of ZnAl₂O₄ spinel.

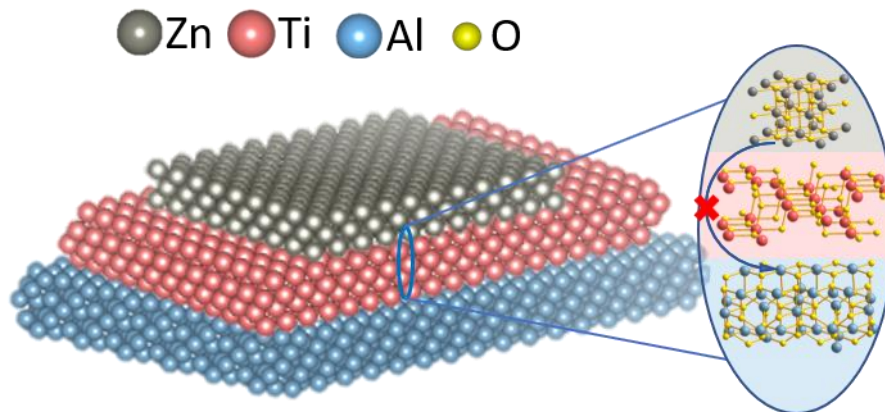


Table 1. RADS performance of TiO₂ modified and unmodified adsorbents with a Zn/Al molar ratio of 1:1 at the breakthrough point (10 ppm Sulfur).

Samples	Breakthrough time/ h	Sulfur capacity/ mg·g ⁻¹	ZnO conversion (%)
Ti-1-1-0	7.00	10.5	7.04
Ti-1-1-3	5.18	7.8	5.22
C-1-1-0	8.10	12.1	7.62
C-1-1-3	1.95	3.8	2.39

An anatase protection layer is introduced into the Ni/ZnO-Al₂O₃ adsorbents via the wet impregnation method to inhibit the formation of inert ZnAl₂O₄. The modified adsorbents show high stability and good desulfurization activity compared with the unmodified adsorbents. The TiO₂ protection layer also provides a certain amount of Lewis acid sites to enhance the adsorption ability of organic sulfur compounds.

Keywords: Ni/ZnO-Al₂O₃ adsorbents; Reactive adsorption desulfurization; Stability; ZnAl₂O₄ spinel; TiO₂.

Bowen Liu, Peng Bai* Yang Wang, Zhun Dong, Pingping Wu, Svetlana Mintova and Zifeng Yan

Highly stable Ni/ZnO-Al₂O₃ adsorbent promoted by TiO₂ for reactive adsorption desulfurization

